Comparison of 2 synthetically generated recombinant prions

Yi Zhang[1,2], Fei Wang[2,†], Xinhe Wang[2,†], Zhihong Zhang[1], Yuanyuan Xu[1], Guohua Yu[1], Chonggang Yuan[1], and Jiyan Ma[1,2,†,*]

[1]Key Laboratory of Brain Functional Genomics; Ministry of Education; Shanghai Key Laboratory of Brain Functional Genomics; School of Life Sciences; East China Normal University; Shanghai, PR China; [2]Department of Molecular and Cellular Biochemistry; Ohio State University; Columbus, OH USA

[†]Current affiliation: Center for Neurodegenerative Science; Van Andel Research Institute; Grand Rapids, MI USA

Prion is a protein-conformation-based infectious agent causing fatal neurodegenerative diseases in humans and animals. Our previous studies revealed that in the presence of cofactors, infectious prions can be synthetically generated in vitro with bacterially expressed recombinant prion protein (PrP). Once initiated, the recombinant prion is able to propagate indefinitely via serial protein misfolding cyclic amplification (sPMCA). In this study, we compared 2 separately initiated recombinant prions. Our results showed that these 2 recombinant prions had distinct biochemical properties and caused different patterns of spongiosis and PrP deposition in inoculated mice. Our findings indicate that various recombinant prions can be initiated in vitro and potential reasons for this variability are discussed.

Introduction

Prion is a protein-conformation-based infectious agent that causes transmissible spongiform encephalopathies (TSEs, also known as prion disease) in animals and humans.[1,2] The prion hypothesis posits that the pathogenic conformer of host encoded prion protein (PrP) is able to convert host PrP to the pathogenic conformation.[1,3] It is well established that the pathogenic PrP^{Sc} conformer is β-sheeted, aggregated, and protease-resistant, which distinctly differs from the α-helical, soluble, and protease-sensitive normal PrP^{C} conformer.[4] The most widely used biochemical property separating these 2 PrP conformers is the sensitivity to proteinase K (PK) digestion. PrP^{C} is sensitive to PK digestion, whereas the C-terminus of PrP^{Sc} is highly resistant to PK digestion resulting in a characteristic C-terminal PK-resistant core.[4,5]

The association of the PK-resistant PrP^{Sc} conformer and prion infectivity was established by the development of serial protein misfolding cyclic amplification (sPMCA) technique, which consists of alternating cycles of sonication and incubation.[6-8] Using normal brain homogenate as substrate for sPMCA, Castilla et al. demonstrated that PrP^{Sc} is able to seed PrP^{C} conversion to the PK-resistant PrP^{Sc} conformation and more importantly, the prion

infectivity is propagated along with the propagation of PrP^{Sc} conformers.[8] Recently, the same sPMCA technique has been successfully applied to propagate the pathogenic PrP^{Sc} conformer and prion infectivity using a variety of native or recombinant PrP substrates.[9-18]

Although sPMCA was originally developed as a technique to propagate the pathogenic PrP^{Sc} conformer,[6,7] several studies showed that it also has the capability to initiate the pathogenic PrP^{Sc} conformation de novo in unseeded reactions.[9,11,15,19] Using sPMCA with a substrate system consisting of purified bacterially-expressed recombinant murine PrP (rPrP) plus synthetic phospholipid POPG (1-palmitoyl-2-oleoylphosphatidylglycerol) and total RNA isolated from normal mouse liver as cofactors, we previously reported de novo formation of a PK-resistant and highly infectious prion in the laboratory of Ohio State University (named as rPrP-res^{OSU}).[9] To confirm this result, we repeated the same experiment in a newly established lab in East China Normal University that has never been exposed to any naturally occurring prion. An infectious prion with a 17 kDa PK-resistant core was generated de novo during this attempt, which was named as rPrP-res^{17kDa}.[11] Both rPrP-res^{OSU} and rPrP-res^{17kDa} have the characteristic self-perpetuating C-terminal PK-resistant conformation
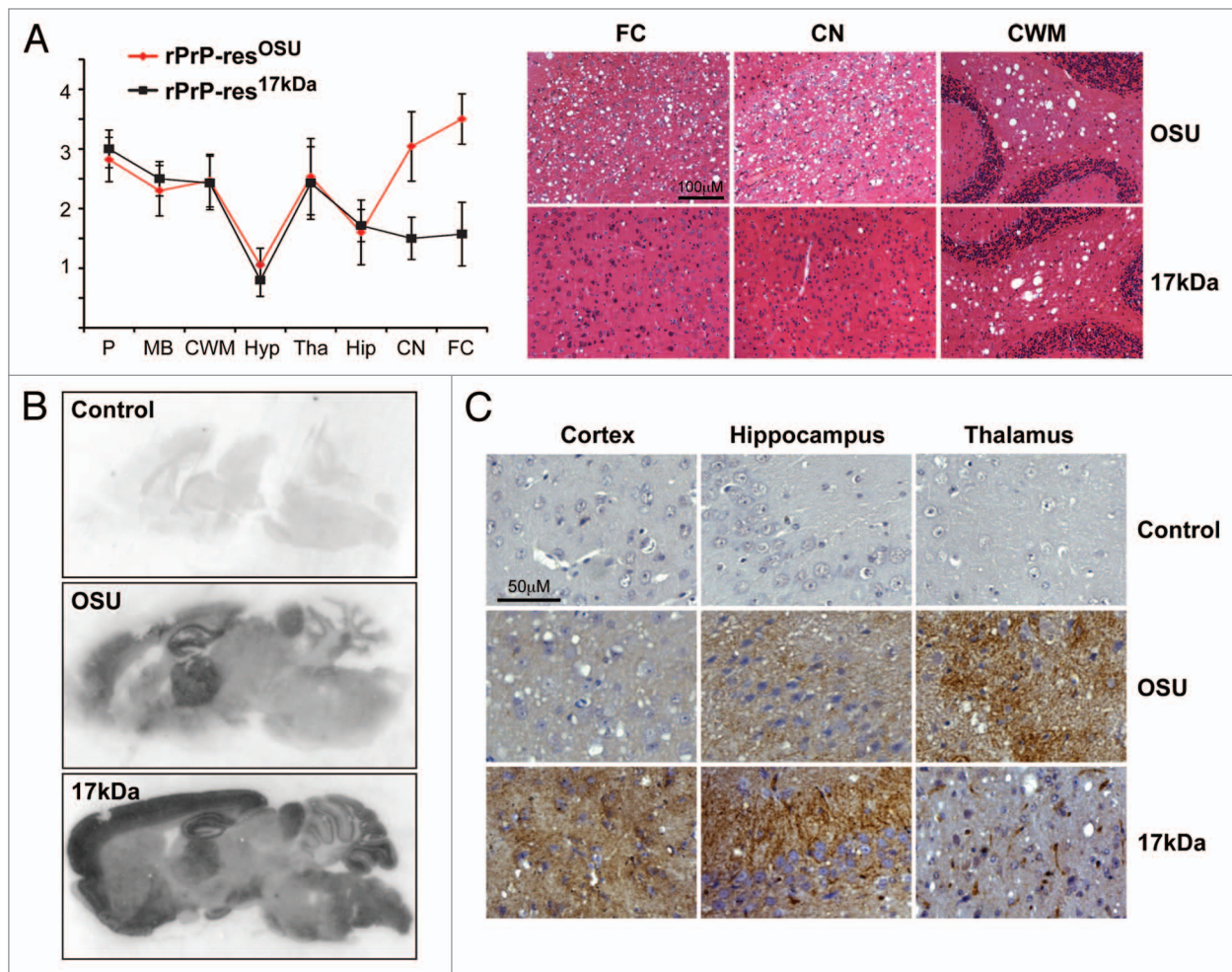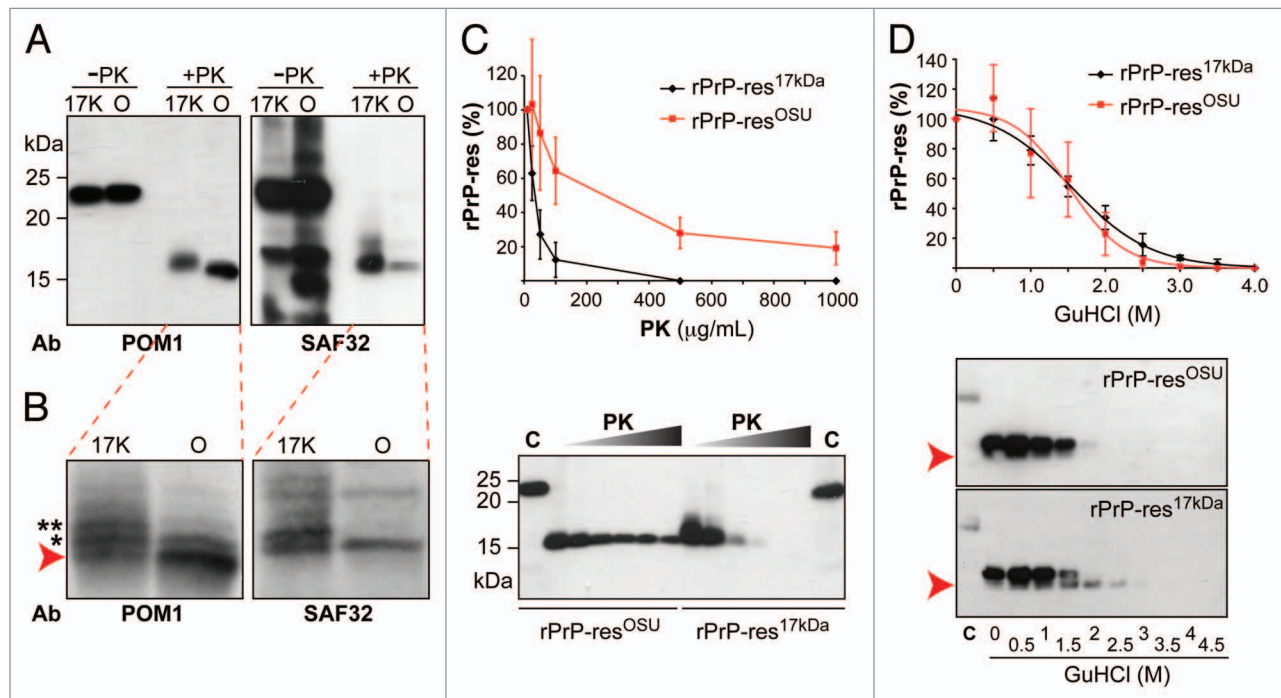
Figure 1. Pathological comparison of rPrP-res[17kDa]- and rPrP-res[OSU]-inoculated mice. (**A**) Lesion profile of spongiosis and representative images of HE staining of mice inoculated with rPrP-res[17kDa] (17kDa) or rPrP-res[OSU] (OSU) as indicated. P, pons; MB, middle brain; CWM, cerebellum white matter; Hyp, hypothalamus; Tha, thalamus; Hip, hippocampus; CN, caudate nucleus; FC, frontal cortex. The lesion profile was based on the scores of 6 rPrP-res[17kDa]-inoculated and 15 rPrP-res[OSU]-inoculated mice. Units of Y-axis are arbitrary units of lesion severity, which are described in detail in methods section. Representative images of spongiosis in frontal cortex (FC), caudate nucleus (CN), and cerebellum white matter (CWM) are shown in (**A**). (**B**) PET blot analysis of mice inoculated with rPrP-res[17kDa] (17kDa) or rPrP-res[OSU] (OSU) as indicated. PET blots were stained at the same time and using exactly the same condition. Three pairs of mice inoculated with rPrP-res[17kDa] or rPrP-res[OSU] were subjected to PET blot analysis and PK-resistant PrP deposition pattern was consistent within the same group. (**C**) Immunohistochemical staining of aberrant PrP deposit in various regions of mouse brain receiving intracerebral inoculation of rPrP-res[17kDa] (17kDa) or rPrP-res[OSU] (OSU) as indicated. Mice receiving control inoculum (PBS + BSA) were used as controls in all panels (Control). These sections were stained at the same time and using exactly the same condition. Three pairs of mice inoculated with rPrP-res[17kDa] or rPrP-res[OSU] were analyzed and the aberrant PrP deposition pattern was consistent within the same group.

and cause fatal prion disease in wild-type mice with 100% attack rate.[9,11] Mice inoculated with rPrP-res[OSU] or rPrP-res[17kDa] survived for 150 or 172 dpi (days post inoculation) respectively,[9,11] which are in the range of survival times for naturally occurring mouse prions. To determine the similarity and/or difference between these 2 separately initiated recombinant prions, we compared the neuropathology caused by these 2 recombinant prions and their biochemical properties in this study.

Results

Pathological change in prion disease is characterized by the presence of vacuoles (spongiosis) in diseased brains. Both rPrP-res[OSU] and rPrP-res[17kDa] caused wide spread spongiosis in wild-type CD-1 mice.[9,11] Interestingly, the spongiosis profile in rPrP-res[17kDa]-inoculated mice appeared to be different from that of rPrP-res[OSU] (**Fig. 1A**). The most prominent differences of spongiosis were observed in frontal cortex (FC) and caudate nucleus (CN). Severe spongiosis was observed in both FC and CN areas of rPrP-res[OSU]-inoculated mice, but only mild spongiosis was detected in these 2 areas of rPrP-res[17kDa]-inoculated mice (**Fig. 1A**). The severity of spongiosis in other brain areas, such as cerebellum white matter (CWM), was very similar (**Fig. 1A**). To determine whether rPrP-res[17kDa] and rPrP-res[OSU] led to different aberrant PrP deposition patterns in the brain, we performed paraffin-embedded tissue (PET) blot and immunohistochemical (IHC) staining. The PET blot revealed a drastic difference

Figure 2. Biochemical comparison of rPrP-res[17kDa] and rPrP-res[OSU]. (**A**) The rPrP-res[17kDa] (17K) and rPrP-res[OSU] (O) with or without PK digestion were subjected to immunoblot analysis with POM1 and SAF32 antibodies as indicated. (**B**) Images obtained by scanning the blots in (A) with a Storm 860 PhosphorImager. Arrow indicates the PK resistant band with smallest molecular weight. Asterisks (* and **) indicate the 2 slower migrating PK-resistant bands. (**C**) The rPrP-res[17kDa] and rPrP-res[OSU] were digested with 10, 25, 50, 100, 500, and 1000 μg/mL PK at 37 °C for 30 min. The PK-resistant rPrP-res was detected by immunoblot analysis with POM1 antibody. The curve represents the average of 4 independent experiments and the error bar represents standard deviation. All immunoblot analyses showed similar patterns and a representative image was presented here. C, undigested control samples. (**D**) The rPrP-res[17kDa] and rPrP-res[OSU] were treated with 0, 0.5, 1, 1.5, 2, 2.5, 3, 3.5, and 4 M GuHCl for 1 h, and then digested with 10 μg/mL PK at 37 °C for 30 min. The rPrP-res was detected by immunoblot analysis with POM1 antibody. The curve represents the average of 3 independent experiments and the error bar represents standard deviation. Arrow indicates the position of the smaller rPrP band, which was consistently detected in all 3 experiments.

in PK-resistant PrP deposition in cortex. Compared with that in rPrP-res[OSU]-inoculated mice, the cortical PK-resistant PrP deposition was much stronger in rPrP-res[17kDa]-inoculated mice (**Fig. 1B**). The IHC staining confirmed the difference in PrP deposition in cortex (**Fig. 1C**, left panel). Moreover, IHC staining also revealed that, compared with rPrP-res[OSU]-inoculated mouse brains, the rPrP-res[17kDa] inoculation caused a stronger PrP deposition in hippocampus, but a weaker PrP deposition in thalamus (**Fig. 1C**, middle and right panels). Together, neuropathological comparison revealed a clear difference between the disease pathologies caused by rPrP-res[17kDa] and rPrP-res[OSU].

Since the bioassays of rPrP-res[17kDa] and rPrP-res[OSU] were performed in outbred CD-1 mice in 2 different animal facilities, the observed difference in disease pathology could be resulted from a variety of factors such as the differences in mouse genetic background. However, it is also possible that rPrP-res[17kDa] and rPrP-res[OSU] are different rPrP conformers, which contributes to the difference in disease pathology. To test the latter possibility, we compared the biochemical properties of rPrP-res[17kDa] and rPrP-res[OSU].

Immunoblot analysis with POM1 antibody that recognizes an epitope at C-terminus of PrP[20,21] showed that the sizes of the PK-resistant fragments of 2 rPrP-res forms were similar, but the PK-resistant core of rPrP-res[17kDa] was slightly larger than that of

rPrP-res[OSU] (**Fig. 2A**, left panel). When immunoblot analysis was performed with SAF32 antibody that recognizes the N-terminal octarepeat region,[22] a much stronger signal was detected with PK-digested rPrP-res[17kDa] (+PK, **Fig. 2A**, right panel). The immunoblot analysis of control samples with SAF32 antibody (−PK, **Fig. 2A**, right panel) showed comparable intensity, indicating that there is no significant difference between the affinity of SAF32 antibody to rPrP-res[17kDa] and rPrP-res[OSU]. Thus, a weaker signal of the PK-resistant fragment of rPrP-res[OSU] (+PK, **Fig. 2A**, right panel) suggests that rPrP-res[17kDa] contains a longer PK-resistant core(s), which extends into the octarepeat region resulting in a better SAF32 antibody detection.

When the same blots were scanned by a Storm 860 PhosphorImager that holds a wider detection range than X-ray film, multiple PK-resistant bands were recognizable in both rPrP-res[17kDa] and rPrP-res[OSU] samples (**Fig. 2B**). For rPrP-res[OSU], 2 major PK-resistant bands were detected by POM-1 antibody and the most abundant band was the one with smallest molecular weight (**Fig. 2B**, indicated by an arrow), whereas for rPrP-res[17kDa], 3 major PK-resistant bands were detected by POM-1 antibody and the most abundant bands were the 2 slower migrating bands (**Fig. 2B**, indicated by * and ** on left panel). In addition to the band intensity, a slight difference in band size was also observed (**Fig. 2B**, the band with evident size difference was indicated by

** on left panel). The SAF32 antibody recognized slower migrating PK-resistant bands but not the one with smallest molecular weight (**Fig. 2B**, right panel), accounting for its weaker recognition of PK-resistant bands of rPrP-res[OSU] (**Fig. 2A**, right panel). Together, these results indicate that the PK cleavage sites in rPrP-res are heterogeneous, which is similar to that of naturally occurring PrP[Sc].[5]

A possible reason for the banding pattern difference between rPrP-res[17kDa] and rPrP-res[OSU] (**Fig. 2B**, left panel) could be due to an insufficient PK digestion of the rPrP-res[17kDa]. To test this possibility, we performed serial PK digestion of 2 samples. We first normalized rPrP-res[17kDa] and rPrP-res[OSU] to similar amount of total rPrP (2 controls in the lower panel of **Fig. 2C**); confirmed by PhosphorImager quantification (the difference between the average of raw PhosphorImager quantification scores for these 2 controls was less than 1%). After being normalized, samples were digested with increasing amounts of PK and the PK-resistant bands of rPrP-res[17kDa] disappeared at PK concentration of 500 μg/mL. The rPrP-res[OSU], however, showed a much higher PK-resistance and its PK-resistant fragment was clearly detectable after a 30 min 1000 μg/mL PK digestion at 37 °C (**Fig. 2C**). Thus, the banding pattern difference between rPrP-res[17kDa] and rPrP-res[OSU] (**Fig. 2B**, left panel) is not due to insufficient PK digestion of rPrP-res[17kDa]. A more plausible explanation could be that the 2 recombinant prions produce different PK-resistant bands.

Next, we performed the guanidine hydrochloride (GuHCl) denaturation assay to compare the stability of rPrP-res[17kDa] and rPrP-res[OSU]. **Figure 2D** shows that the denaturation curves for rPrP-res[17kDa] and rPrP-res[OSU] were very similar, with $[\text{GuHCl}]_{1/2}$ (the GuHCl concentration causing loss of half of the PK-resistant PrP signal) at 1.51 M for rPrP-res[OSU] and 1.55 M for rPrP-res[17kDa]. Despite the similarity in denaturation curve, the rPrP banding patterns after GuHCl treatment were clearly different between 2 rPrP-res forms. In rPrP-res[17kDa], a smaller PK-resistant fragment became prominent after 1.5 M GuHCl treatment and remained detectable when the concentration of GuHCl was at 2 or 2.5 M (**Fig. 2D**, pointed by an arrow in the bottom rPrP-res[17kDa] panel). In contrast, this smaller PK-resistant fragment was not clearly detected in rPrP-res[OSU] samples (**Fig. 2D**, the rPrP-res[OSU] panel).

Collectively, our biochemical analyses clearly showed that, despite the similar self-perpetuating PK-resistant conformation and similar capability of causing prion disease in wild-type mice, the rPrP-res[17kDa] and rPrP-res[OSU] have distinct differences in biochemical properties.

Discussion

Our 2 successful attempts to generate de novo recombinant prions by sPMCA, particularly the latter attempt conducted in a lab that has never exposed to any naturally occurring prions, support that an infectious recombinant prion can be synthetically generated in vitro. The current comparative study of separately initiated rPrP-res[OSU] and rPrP-res[17kDa] suggests that the 2 recombinant prions are differently misfolded rPrPs, with distinct biochemical

properties and causing different neuropathological changes. The sPMCA substrate mixtures for de novo formation of rPrP-res[OSU] and rPrP-res[17kDa] contained the same 3 components: recombinant murine PrP, POPG, and total RNA isolated from normal mouse liver. Despite the relatively simple components in the substrate mixture, many variations may lead to the differences in de novo generated, self-perpetuating PK-resistant rPrP-res forms.

First, depending on the metabolic status of the mouse, the total RNA isolated from each individual mouse liver may contain different RNA species with different three-dimensional RNA structures. Moreover, purification of total RNA is always accompanied with co-purified molecules, which may also vary according to the metabolic status of individual mouse. Therefore, despite the same reagent and protocol, the isolated total RNA may vary from mouse to mouse. Our recent study has shown that variations in RNA species or co-purified molecules are not essential for generating the rPrP-res conformation and prion infectivity.[10] However, it does not preclude the potential difference in modulating rPrP-res conformation by different RNA species or co-purified molecules.

Second, the differences in rPrP-res forms may result from different ratios of rPrP and cofactors. Thus far, it remains unclear whether cofactors are in the final rPrP-res complex.[23,24] Even if cofactors play a chaperone-like role to facilitate rPrP-res formation, different rPrP:cofactors ratios may guide rPrP to different misfolding stage and result in rPrP-res conformational differences. If cofactors are part of the final rPrP-res complex, variation in rPrP:cofactor ratios will most likely alter the final rPrP three-dimensional structure. If cofactors are not essential for the self-perpetuating capability, then the final rPrP-res complex can be with or without cofactors. In this case, the presence or absence of cofactors may produce different rPrP-res conformations leading to different biological effects. Thus, despite the relatively simple sPMCA substrate system for de novo rPrP-res formation, the possible variations in rPrP:cofactors ratios are enormous, which may contribute to the formation of different rPrP-res form.

Third, the variations in rPrP-res conformation may also result from the sonication step of sPMCA. Previous studies showed that the interaction between rPrP and cofactors (POPG and RNA) in our sPMCA substrate converts rPrP to a β-sheeted, aggregated, and PK-resistant conformation similar to rPrP-res.[24-31] When this substrate is subjected to sPMCA, sonication breaks rPrP aggregates in the substrate (and/or directly alters rPrP conformation) and new rPrP aggregates form during incubation. As we suggested previously,[11] this repeated rPrP aggregate breaking-and-formation cycles may ultimately re-package rPrP into self-perpetuating rPrP-res aggregates. Because of its seeding capability, once initiated, the rPrP-res aggregates can be faithfully propagated via sPMCA. If this model is correct, the power of sonication, such as different sonicators or different tube positions in the sonicator horn, will likely influence the extent of rPrP-res aggregate breakage and/or the level of rPrP conformation alteration, both of which may lead to the variations in the initial rPrP-res conformation.

A fourth explanation for the formation of 2 different forms of rPrP-res could be simply due to the adoption of different stable rPrP-res conformers. The rPrP-res is a misfolded rPrP form and

there could be multiple stable rPrP-res spots in the energy landscape.[32] In this scenario, the presence of cofactors and the sPMCA process may create an environment favoring rPrP conformational change, allowing rPrP to randomly search for the stable spots in the energy landscape. Once rPrP adopts distinct stable rPrP-res conformations, different rPrP-res forms are initiated and propagated.

Any of the above reasons, or combination of them, may contribute to the de novo formation of different rPrP-res forms, which may account for the observation of our current study and the recent reports of various de novo generated non-infectious self-perpetuating rPrP-res forms.[11,33]

It is important to note that although we have shown the biochemical and neuropathological differences between rPrP-res[OSU] and rPrP-res[17kDa], we cannot conclude that these are 2 different prion strains. This is because the mouse bioassays were performed in outbred CD-1 mice in 2 different animal vivaria. Careful serial passage in inbred mouse line is required to clarify this question. Despite the caveats, our observation that the 2 forms of rPrP-res produce heterogeneous PK-resistant rPrP species (**Fig. 2B**) is consistent with the quasispecies theory,[32,34] which posits that a prion strain consists of an ensemble of PrP^{Sc} conformers, and various prion strains may differ in certain or all PrP^{Sc} species in the group and/or the proportion of each PrP^{Sc} species.

Results from our comparison study clearly showed that different rPrP-res forms can be formed de novo, which leads to different disease pathologies in mice. This finding supports that not a single PrP conformer, but multiple PrP conformers are capable of supporting prion infectivity.

Materials and Methods

PET blot was performed as previously described.[9,35] Briefly, 4-μm-thick paraffin sections were collected onto 0.45-μm nitrocellulose membranes (Bio-Rad Laboratories) and incubated at 55 °C for 16 h. Membranes were dewaxed by immersion in xylene (45 °C, 20 min) and rinsed in isopropanol (2 × 10 min) followed by stepwise rehydration. After washing with tris-buffered saline buffer (TBST, 50 mM TRIS-HCl, 150 mM NaCl, pH 8.0, 0.1% Tween-20), the membrane was subjected to 250 μg/mL PK digestion in a buffer consisting of 10 mM TRIS-HCl, pH 7.8, 100 mM NaCl, 0.1% Brij 35 for 16 h at 55 °C. After washing with TBST, the membrane was treated with 4 M guanidine thiocyanate for 10 min and washed 3 times in TBST. The membrane was blocked by 2% non-fat milk in TBST for 1 h, incubated with monoclonal SAF84 anti-PrP antibody (1:2000 in blocking solution) for 90 min at room temperature, washed 3 times in TBST, and incubated with an AP conjugated goat anti-mouse IgG antibody (1:3000 in blocking solution) for 1 h at room temperature. After 3 washes with TBST, the color was developed by BCIP/NBT, and the images were assessed using a stereomicroscope.

Histopathological analyses were performed as previously described.[9,36,37] The lesion profile of spongiosis was determined using the following standard: 0, no vacuolation; 0.5, minimum vacuolation (>1 vacuole per field under 20× magnification); 1, little vacuolation (<10 vacuoles per field under 20× magnification); 2, moderate vacuolation (many vacuoles in a field under 20× magnification); 3, extensive vacuolation (numerous vacuoles in a field under 20× magnification); 4, severe vacuolation (vacuoles all over the field and often coalescing).

GuHCl denaturation assay was performed by mixing 30 μL sPMCA product with 30 μL GuHCl stock solutions to reach final GuHCl concentrations ranging from 0 to 4 M. The mixtures were incubated at room temperature for 1 h and mixed by vortexing every 15 min. Afterwards, samples were kept on ice and stock solutions were added to normalize the final salt and detergent concentrations to: 0.4 M GuHCl, 0.15% Triton X-100, 16.5 mM TRIS-HCl, pH 7.4 and 7.5 mM NaCl. Normalized samples were digested with PK (10 μg/mL) for 30 min at 37 °C. Digestion was terminated by adding 1 mM PMSF and incubation on ice for 5 min. PK-resistant proteins were precipitated by adding 4 volumes of cold methanol (–20 °C) and incubated at –20 °C for 30 min. The precipitated proteins were pelleted by centrifugation, resuspended in SDS-PAGE sample buffer, subjected to immunoblot analysis, and the results were quantified by scanning with a Storm 860 PhosphorImager.

Immunoblot analysis was performed as previously described.[37] The blot was developed with ECL-plus reagent (GE Healthcare Life Science) and the signal was detected by exposure to X-ray film or scanning with a Storm 860 PhosphorImager (**Fig. 2B**).

Reagents used in this study include Polyvinylidene Fluoride (PVDF) membrane and ECL-plus reagent (GE Healthcare Life Science), Proteinase K (Lyophilizate, recombinant, PCR grade) (Roche), Phenylmethanesulfonyl fluoride (PMSF) (Sigma-Aldrich). Other chemicals were purchased from Sango Biotech Co. Ltd. or Fisher Scientific Inc. Antibodies used in this study include SAF32 and SAF-84 anti-PrP antibodies (Cayman Chemical), POM1 anti-PrP antibody (a generous gift from Dr Adriano Aguzzi), HRP-conjugated goat anti-mouse IgG antibody (Bio-Rad).

References

1. Prusiner SB. Prions. Proc Natl Acad Sci U S A 1998; 95:13363-83; PMID:9811807; http://dx.doi.org/10.1073/pnas.95.23.13363

2. Aguzzi A, Sigurdson C, Heikenwaelder M. Molecular mechanisms of prion pathogenesis. Annu Rev Pathol 2008; 3:11-40; PMID:18233951; http://dx.doi.org/10.1146/annurev.pathmechdis.3.121806.154326

3. Prusiner SB. Novel proteinaceous infectious particles cause scrapie. Science 1982; 216:136-44; PMID:6801762; http://dx.doi.org/10.1126/science.6801762

4. Caughey B, Chesebro B. Prion protein and the transmissible spongiform encephalopathies. Trends Cell Biol 1997; 7:56-62; PMID:17708907; http://dx.doi.org/10.1016/S0962-8924(96)10054-4

5. Parchi P, Zou W, Wang W, Brown P, Capellari S, Ghetti B, Kopp N, Schulz-Schaeffer WJ, Kretzschmar HA, Head MW, et al. Genetic influence on the structural variations of the abnormal prion protein. Proc Natl Acad Sci U S A 2000; 97:10168-72; PMID:10963679; http://dx.doi.org/10.1073/pnas.97.18.10168

6. Saborio GP, Permanne B, Soto C. Sensitive detection of pathological prion protein by cyclic amplification of protein misfolding. Nature 2001; 411:810-3; PMID:11459061; http://dx.doi.org/10.1038/35081095

7. Castilla J, Saá P, Morales R, Abid K, Maundrell K, Soto C. Protein misfolding cyclic amplification for diagnosis and prion propagation studies. Methods Enzymol 2006; 412:3-21; PMID:17046648; http://dx.doi.org/10.1016/S0076-6879(06)12001-7

8. Castilla J, Saá P, Hetz C, Soto C. In vitro generation of infectious scrapie prions. Cell 2005; 121:195-206; PMID:15851027; http://dx.doi.org/10.1016/j.cell.2005.02.011

9. Wang F, Wang X, Yuan CG, Ma J. Generating a prion with bacterially expressed recombinant prion protein. Science 2010; 327:1132-5; PMID:20110469; http://dx.doi.org/10.1126/science.1183748

10. Wang F, Zhang Z, Wang X, Li J, Zha L, Yuan CG, Weissmann C, Ma J. Genetic informational RNA is not required for recombinant prion infectivity. J Virol 2012; 86:1874-6; PMID:22090130; http://dx.doi.org/10.1128/JVI.06216-11

11. Zhang Z, Zhang Y, Wang F, Wang X, Xu Y, Yang H, Yu G, Yuan C, Ma J. De novo generation of infectious prions with bacterially expressed recombinant prion protein. FASEB J 2013; 27:4768-75; PMID:23970796; http://dx.doi.org/10.1096/fj.13-233965

12. Kim JI, Cali I, Surewicz K, Kong Q, Raymond GJ, Atarashi R, Race B, Qing L, Gambetti P, Caughey B, et al. Mammalian prions generated from bacterially expressed prion protein in the absence of any mammalian cofactors. J Biol Chem 2010; 285:14083-7; PMID:20304915; http://dx.doi.org/10.1074/jbc.C110.113464

13. Deleault NR, Piro JR, Walsh DJ, Wang F, Ma J, Geoghegan JC, Supattapone S. Isolation of phosphatidylethanolamine as a solitary cofactor for prion formation in the absence of nucleic acids. Proc Natl Acad Sci U S A 2012; 109:8546-51; PMID:22586108; http://dx.doi.org/10.1073/pnas.1204498109

14. Deleault NR, Walsh DJ, Piro JR, Wang F, Wang X, Ma J, Rees JR, Supattapone S. Cofactor molecules maintain infectious conformation and restrict strain properties in purified prions. Proc Natl Acad Sci U S A 2012; 109:E1938-46; PMID:22711839; http://dx.doi.org/10.1073/pnas.1206999109

15. Deleault NR, Harris BT, Rees JR, Supattapone S. Formation of native prions from minimal components in vitro. Proc Natl Acad Sci U S A 2007; 104:9741-6; PMID:17535913; http://dx.doi.org/10.1073/pnas.0702662104

16. Geoghegan JC, Miller MB, Kwak AH, Harris BT, Supattapone S. Trans-dominant inhibition of prion propagation in vitro is not mediated by an accessory cofactor. PLoS Pathog 2009; 5:e1000535; PMID:19649330; http://dx.doi.org/10.1371/journal.ppat.1000535

17. Gonzalez-Montalban N, Makarava N, Ostapchenko VG, Savtchenk R, Alexeeva I, Rohwer RG, Baskakov IV. Highly efficient protein misfolding cyclic amplification. PLoS Pathog 2011; 7:e1001277; PMID:21347353; http://dx.doi.org/10.1371/journal.ppat.1001277

18. Imamura M, Kato N, Yoshioka M, Okada H, Iwamaru Y, Shimizu Y, Mohri S, Yokoyama T, Murayama Y. Glycosylphosphatidylinositol anchor-dependent stimulation pathway required for generation of baculovirus-derived recombinant scrapie prion protein. J Virol 2011; 85:2582-8; PMID:21228241; http://dx.doi.org/10.1128/JVI.02098-10

19. Barria MA, Mukherjee A, Gonzalez-Romero D, Morales R, Soto C. De novo generation of infectious prions in vitro produces a new disease phenotype. PLoS Pathog 2009; 5:e1000421; PMID:19436715; http://dx.doi.org/10.1371/journal.ppat.1000421

20. Polymenidou M, Moos R, Scott M, Sigurdson C, Shi YZ, Yajima B, Hafner-Bratkovic I, Jerala R, Hornemann S, Wuthrich K, et al. The POM monoclonals: a comprehensive set of antibodies to non-overlapping prion protein epitopes. PLoS One 2008; 3:e3872; PMID:19060956; http://dx.doi.org/10.1371/journal.pone.0003872

21. Baral PK, Wieland B, Swayampakula M, Polymenidou M, Rahman MH, Kav NN, Aguzzi A, James MN. Structural studies on the folded domain of the human prion protein bound to the Fab fragment of the antibody POM1. Acta Crystallogr D Biol Crystallogr 2012; 68:1501-12; PMID:23090399; http://dx.doi.org/10.1107/S0907444912037328

22. Féraudet C, Morel N, Simon S, Volland H, Frobert Y, Créminon C, Vilette D, Lehmann S, Grassi J. Screening of 145 anti-PrP monoclonal antibodies for their capacity to inhibit PrPSc replication in infected cells. J Biol Chem 2005; 280:11247-58; PMID:15618225; http://dx.doi.org/10.1074/jbc.M407006200

23. Ma J. The role of cofactors in prion propagation and infectivity. PLoS Pathog 2012; 8:e1002589; PMID:22511864; http://dx.doi.org/10.1371/journal.ppat.1002589

24. Wang F, Ma J. Role of lipid in forming an infectious prion? Acta Biochim Biophys Sin (Shanghai) 2013; 45:485-93; PMID:23583976; http://dx.doi.org/10.1093/abbs/gmt038

25. Wang F, Yang F, Hu Y, Wang X, Wang X, Jin C, Ma J. Lipid interaction converts prion protein to a PrPSc-like proteinase K-resistant conformation under physiological conditions. Biochemistry 2007; 46:7045-53; PMID:17503780; http://dx.doi.org/10.1021/bi700299h

26. Wang F, Yin S, Wang X, Zha L, Sy MS, Ma J. Role of the highly conserved middle region of prion protein (PrP) in PrP-lipid interaction. Biochemistry 2010; 49:8169-76; PMID:20718504; http://dx.doi.org/10.1021/bi101146v

27. Kazlauskaite J, Pinheiro TJ. Aggregation and fibrillization of prions in lipid membranes. Biochem Soc Symp 2005; 211-22; PMID:15649144

28. Kazlauskaite J, Sanghera N, Sylvester I, Vénien-Bryan C, Pinheiro TJ. Structural changes of the prion protein in lipid membranes leading to aggregation and fibrillization. Biochemistry 2003; 42:3295-304; PMID:12641461; http://dx.doi.org/10.1021/bi026872q

29. Morillas M, Swietnicki W, Gambetti P, Surewicz WK. Membrane environment alters the conformational structure of the recombinant human prion protein. J Biol Chem 1999; 274:36859-65; PMID:10601237; http://dx.doi.org/10.1074/jbc.274.52.36859

30. Adler V, Zeiler B, Kryukov V, Kascsak R, Rubenstein R, Grossman A. Small, highly structured RNAs participate in the conversion of human recombinant PrP(Sen) to PrP(Res) in vitro. J Mol Biol 2003; 332:47-57; PMID:12946346; http://dx.doi.org/10.1016/S0022-2836(03)00919-7

31. Gomes MP, Millen TA, Ferreira PS, e Silva NL, Vieira TC, Almeida MS, Silva JL, Cordeiro Y. Prion protein complexed to N2a cellular RNAs through its N-terminal domain forms aggregates and is toxic to murine neuroblastoma cells. J Biol Chem 2008; 283:19616-25; PMID:18456654; http://dx.doi.org/10.1074/jbc.M802102200

32. Li J, Browning S, Mahal SP, Oelschlegel AM, Weissmann C. Darwinian evolution of prions in cell culture. Science 2010; 327:869-72; PMID:20044542; http://dx.doi.org/10.1126/science.1183218

33. Timmes AG, Moore RA, Fischer ER, Priola SA. Recombinant prion protein refolded with lipid and RNA has the biochemical hallmarks of a prion but lacks in vivo infectivity. PLoS One 2013; 8:e71081; http://dx.doi.org/10.1371/journal.pone.0071081; PMID:23936256

34. Collinge J, Clarke AR. A general model of prion strains and their pathogenicity. Science 2007; 318:930-6; PMID:17991853; http://dx.doi.org/10.1126/science.1138718

35. Schulz-Schaeffer WJ, Tschöke S, Kranefuss N, Dröse W, Hause-Reitner D, Giese A, Groschup MH, Kretzschmar HA. The paraffin-embedded tissue blot detects PrP(Sc) early in the incubation time in prion diseases. Am J Pathol 2000; 156:51-6; PMID:10623653; http://dx.doi.org/10.1016/S0002-9440(10)64705-0

36. Wang X, Bowers SL, Wang F, Pu XA, Nelson RJ, Ma J. Cytoplasmic prion protein induces forebrain neurotoxicity. Biochim Biophys Acta 2009; 1792:555-63; PMID:19281844; http://dx.doi.org/10.1016/j.bbadis.2009.02.014

37. Wang F, Wang X, Ma J. Conversion of bacterially expressed recombinant prion protein. Methods 2011; 53:208-13; PMID:21176786; http://dx.doi.org/10.1016/j.ymeth.2010.12.013